

PHYSICAL CONDITIONS OF H II REGIONS IN M101 AND THE PREGALACTIC HELIUM ABUNDANCE

S. TORRES-PEIMBERT,¹ M. PEIMBERT,¹ AND J. FIERRO
 Instituto de Astronomía, Universidad Nacional Autónoma de México
 Received 1988 December 15; accepted 1989 March 29

ABSTRACT

Spectrophotometry in the 3400–7400 Å range is presented for eight H II regions and the nucleus of M101. The He, N, O, Ne, S, and Ar abundances relative to H are derived. The O/H ratios are smaller than previously found by about 0.2 dex. We find negative gradients with galactocentric distance of the O/H, N/O, and He/H ratios. We do not find any gradients in the S/O, Ne/O, and Ar/O ratios. The pregalactic helium abundance by mass has been determined from NGC 2363, NGC 5471, and the SMC H II regions and amounts to 0.230 ± 0.006 (1 σ).

Subject headings: galaxies: individual (M101) — galaxies: nuclei — nebulae: abundances — nebulae: H II regions

I. INTRODUCTION

M101 (NGC 5457) is a nearby grand design Sc galaxy, with very prominent H II regions. There are in the literature high-quality spectroscopic observations of the brightest H II regions (Peimbert and Spinrad 1970; Searle 1971; Searle and Sargent 1972; Smith 1975; Shields and Searle 1978; Sedwick and Aller 1981; Rayo, Peimbert, and Torres-Peimbert 1982; McCall, Rybski, and Shields 1985).

We present photoelectric studies of eight H II regions and the nucleus in this galaxy, taken during six observing seasons, spread over nine years, in order to redetermine their physical parameters and chemical composition, in particular to derive their helium abundance, taking into account the nonlinearity of the IDS detector.

For this work we have adopted a distance of 7.4 Mpc to M101 (Sandage and Tammann 1976; with the suggested correction by de Vaucouleurs 1978), an inclination angle relative to the plane of the sky of 27°, a position angle of the line of nodes of 30°, and an isophotal radius of 12:3 (corresponding to 26.5 kpc). In § II we present the observations, in § III we determine ionic and total chemical abundances, and in § IV we discuss our results and their implications.

II. OBSERVATIONS

The observed H II regions are presented in Table 1, along with their offset positions from the galactic nucleus, in arcseconds. Observation dates and galactocentric distances corrected for the inclination angle are also given.

The observations were carried out with the 2.1 m telescope at KPNO, with the Gold spectrograph and the intensified image dissector scanner (IDS). The observational procedure has been described by Torres-Peimbert and Peimbert (1977).

Four gratings were used that covered the following wavelength ranges: $\lambda\lambda 3400\text{--}5200$, $\lambda\lambda 5600\text{--}7400$, $\lambda\lambda 5850\text{--}6750$, and $\lambda\lambda 4800\text{--}6600$. The dual entrance slits used were 0.30×0.98 mm where the first value is along and the second is perpendicular to the dispersion; they correspond to $3''.8 \times 12''.4$ on the

plane of the sky. The separation between the center of the slits was 99" on the sky. The slit was centered on the brightest part of the objects; each object was observed alternating both slits. Each beam was treated independently and in all cases the sky was subtracted from the source. The sky measurements were made outside the body of M101. The IDS is a dual-beam multichannel spectrometer; each spectrum of roughly 20 mm is recorded into 1024 channels. The width at half-maximum (FWHM) was of 3.8 channels.

The data were reduced to absolute fluxes using the standard stars observed by Stone (1977) and Oke (1974) and correcting for the nonlinearity of the detector by considering that the actual flux, F , is related to the instrumental signal, S , as determined by Peimbert and Torres-Peimbert (1987a)

$$S \propto F^{1.07}. \quad (1)$$

In Table 2 we present the intrinsic line intensities in ergs $\text{cm}^{-2} \text{s}^{-1}$, $I(\lambda)$, given by

$$\log [I(\lambda)/I(\text{H}\beta)] = \log [F(\lambda)/F(\beta)] + C(\text{H}\beta)f(\lambda), \quad (2)$$

where $F(\lambda)$ is the observed line flux corrected for atmospheric extinction and $C(\text{H}\beta)$ is the logarithmic reddening correction at $\text{H}\beta$. For the nucleus, only $F(\lambda)$ values are given. The line intensities have not been corrected for underlying absorption. The reddening function, $f(\lambda)$, normalized to $\text{H}\beta$ is derived from the normal extinction law (Whiteford 1958). The $C(\text{H}\beta)$ value was obtained by fitting the observed Balmer decrement with the theoretical one computed by Hummer and Storey (1987), which is very similar to that computed by Brocklehurst (1971), for $T_e = 10,000$ K and $N_e = 100 \text{ cm}^{-3}$. The continuum contribution for each emission line was subtracted and was estimated by interpolating on both sides of the line.

The accuracy of the $F(\text{H}\beta)$ values given in Table 2 is better than 0.06 dex, while that of the $C(\text{H}\beta)$ values is of 0.1 dex for all the objects. In general we observed the brightest part of each H II complex and the positional repeatability was about 1"; the coordinates in Table 1 are taken from the literature.

The standard deviations between the intrinsic line ratios and the theoretical ratios $\text{H}\delta/\text{H}\beta$, $\text{H}\gamma/\text{H}\beta$, and $\text{H}\alpha/\text{H}\beta$ are: 0.01, 0.01, and 0.00 dex, respectively. In Table 3 we present the equivalent widths of the main observed lines given in log W (Å).

¹ Visiting Astronomer, KPNO, National Optical Astronomical Observatories, operated by the Association of Universities for Research in Astronomy, Inc., under contract with the National Science Foundation.

H II REGIONS IN M101

187

TABLE 1
OBSERVED H II REGIONS IN M101

Region ^a	Position ^b	Observation Date	ρ^c/ρ_0	r^d
Nucleus, NGC 5457	000, 000	1978 May, 1987 Mar	0	0
S2, H108 + H111	-068, -090	1978 May, 1987 Mar	0.15	4.0
S3, H40	+160, +021	1978 May, 1979 Mar, 1980 Mar	0.24	6.3
S5	-155, +093	1982 Dec, 1987 Mar	0.27	7.2
H47	+145, -140	1978 May	0.31	8.1
NGC 5461, S7	+252, -107	1978 May, 1979 Mar, 1980 Mar	0.42	11.1
NGC 5455, S10	-101, -388	1985 Mar	0.55	14.6
NGC 5447	-376, -271	1987 Mar	0.64	17.0
NGC 5471, S13	+666, +172	1978 May, 1979 Mar, 1980 Mar 1982 Dec, 1983 May	0.99	26.2

^a S (Searle 1971), H (Hodge 1969).^b α and δ offsets in arcseconds from galactic nucleus (east and north are positive).^c Deprojected distance from center relative to isophotal radius, where we have adopted $\rho_0 = 12/3$, $i = 27^\circ$, and $\Omega = 30^\circ$.^d Deprojected distance from center, in kpc, for a galactic distance $D = 7.4$ Mpc.TABLE 2
LINE INTENSITIES

λ	ident	$F(\lambda)$				$I(\lambda)$					
		$f(\lambda)$	Nucleus	H108+111	H 40	S5	H47	NGC 5461	NGC 5455	NGC 5447	NGC 5471
3727	[O II]	+0.315	+0.12±0.05	-0.06±0.05	+0.41±0.03	+0.32±0.04	+0.24±0.04	+0.33±0.02	+0.49±0.03	+0.32±0.03	+0.12±0.03
3835	H9	+0.282	-1.10±0.06	-1.15±0.05	-1.19±0.07	-1.23±0.07	-1.17±0.05
3869	[Ne III]	+0.268	...	-1.34±0.10	-1.37±0.07	-0.72±0.04	-0.54±0.04	-0.57±0.04	-0.22±0.03
3889	He I + H8	+0.265	-0.69±0.04	-0.91±0.07	...	-0.72±0.04	-0.68±0.04	-0.74±0.04	-0.73±0.04
3967+3970	[Ne III] + H7	+0.235	-0.75±0.05	-0.80±0.06	...	-0.65±0.04	-0.56±0.04	-0.61±0.04	+0.47±0.03
4026	He I	+0.225	-1.76±0.06	-1.69±0.08	-1.75±0.08	-1.79±0.06
4068+4076	[S II]	+0.210	-1.93±0.08	-1.90±0.07	-1.49±0.07	...	-1.88±0.07
4102	H δ	+0.202	...	-0.60±0.04	-0.59±0.02	-0.59±0.04	-0.60±0.03	-0.60±0.02	-0.56±0.03	-0.56±0.03	-0.59±0.02
4340	H γ	+0.135	...	-0.27±0.03	-0.33±0.01	-0.28±0.03	-0.35±0.02	-0.32±0.01	-0.33±0.02	-0.35±0.02	-0.33±0.01
4363	[O III]	+0.132	<-2.53	-1.83±0.04	-1.71±0.06	...	-1.04±0.02
4388	He I	+0.125	-2.27±0.08
4472	He I	+0.105	-1.43±0.04	-1.39±0.03	-1.30±0.04	-1.34±0.04	-1.45±0.03
4658	[Fe III]	+0.050	-2.15±0.08	-2.00±0.07	-1.85±0.08
4686	He II	+0.045	-1.63±0.07	-1.68±0.05	-1.98±0.06
4702	[Fe III]	+0.040	-2.32±0.08
4711+4713	[Ar IV] + He I	+0.035	-2.35±0.08	-1.90±0.05
4740	[Ar IV]	+0.033	-1.81±0.05
4861	H β	+0.000	0.00	0.00	0.00	0.00	0.00	0.00	0.00	0.00	0.00
4922+4931	He I + [O III]	-0.012	-1.99±0.06	-1.89±0.05	-1.94±0.06
4959	[O III]	-0.020	-0.53±0.02	-1.06±0.04	...	+0.01±0.01	+0.03±0.02	+0.11±0.02	+0.32±0.02
5007	[O III]	-0.028	-0.11±0.02	-0.70±0.02	-0.06±0.01	-0.60±0.02	-0.81±0.02	+0.48±0.01	+0.52±0.01	+0.59±0.01	+0.80±0.01
5048	He I	-0.035	-2.84±0.15
5199+5202	[N I]	-0.075	-1.92±0.08	-2.27±0.08	-2.39±0.15
5755	[N II]	-0.190	-2.20±0.10	-2.43±0.08	-2.77±0.15
5876	He I	-0.210	-1.00±0.04	-1.00±0.06	-1.17±0.08	-0.89±0.03	-0.92±0.04	-0.94±0.04	-0.96±0.03
6300	[O I]	-0.285	-1.79±0.05	-1.81±0.05	-1.42±0.06	...	-1.50±0.04
6311	[S III]	-0.290	-2.00±0.07	-1.88±0.05	-1.80±0.06
6364	[O I]	-0.301	-2.29±0.08	-2.30±0.08	-1.96±0.07
6548	[N II]	-0.332	+0.07±0.03	-0.54±0.05	-0.64±0.04	-0.50±0.05	-0.57±0.05	-0.89±0.05	...	-1.06±0.05	-1.57±0.05
6563	H α	-0.335	+1.03±0.02	+0.47±0.03	+0.45±0.02	+0.47±0.03	+0.41±0.03	+0.46±0.01	+0.45±0.02	+0.45±0.02	+0.46±0.02
6584	[N II]	-0.340	+0.59±0.02	-0.06±0.04	-0.17±0.02	-0.04±0.04	-0.10±0.04	-0.44±0.02	-0.48±0.03	-0.61±0.03	-1.05±0.03
6678	He I	-0.360	-1.54±0.06	-1.46±0.05	-1.52±0.06	-1.48±0.06	-1.53±0.05
6717	[S II]	-0.369	-0.07±0.03	-0.48±0.06	-0.79±0.04	-0.41±0.05	-0.56±0.06	-0.91±0.04	-0.58±0.05	-0.76±0.05	-1.01±0.04
6731	[S II]	-0.371	+0.20±0.03	-0.74±0.06	-0.93±0.04	-0.50±0.05	-0.74±0.06	-0.99±0.04	-0.69±0.05	-0.89±0.05	-1.11±0.04
7065	He I	-0.400	-1.92±0.06	-1.57±0.05	-1.62±0.06	...	-1.56±0.05
7136	[Ar III]	-0.412	-1.19±0.05	-1.02±0.05	-1.02±0.06	-0.97±0.06	-1.14±0.05
7320+7330	[O II]	-0.435	-1.71±0.08	-1.40±0.06	-1.14±0.07	...	-1.39±0.06
C(H β)		...	+0.50	+0.50	+0.50	+0.60	+0.60	+0.60	+0.30	+0.20	+0.30
log F(H β)		-14.02	-13.61	-13.02	-13.46	-13.35	-12.46	-12.79	-12.75	-12.59	-12.59

^a Logarithmic intensities relative to H β , where $F(\lambda)$ is the observed value and $I(\lambda)$ is the intrinsic value after correcting for reddening; $f(\lambda)$ is the reddening correction.

TABLE 3
 EQUIVALENT WIDTHS^a

λ	ident	Nucleus	H 108+				NGC	NGC	NGC	NGC
			H 111	H 40	S5	H 47	5461	5455	5447	5471
3727	[O II]	+0.92:	+1.65	+1.76	+1.62	+1.32	+2.23	+2.20	+2.12	+1.92
3835	H9	+0.25	+0.72	+0.54	+0.63	+0.65
3869	[Ne III]	...	+0.30	-0.01	+1.08	+1.21	+1.30	+1.61
3889	He I + H8	+0.70	+0.39	...	+1.09	+1.07	+1.13	+1.10
3967+3970	[Ne III] + H7	+0.66	+0.51	...	+1.19	+1.26	+1.29	+1.38
4026	He I	+0.18	...	+0.21	+0.05
4068+4076	[S II]	-0.51	-0.03	+0.33	...	-0.03
4102	H δ	...	+1.18	+0.86	+0.77	+0.79	+1.38	+1.30	+1.42	+1.27
4340	H γ	...	+1.38	+1.19	+1.17	+1.15	+1.65	+1.61	+1.70	+1.62
4363	[O III]	+0.14	+0.23	...	+0.91
4388	He I	-0.20
4472	He I	+0.11	+0.71	+0.71	+0.77	+0.52
4658	[Fe III]	-0.52	+0.08	+0.22
4686	He II	-0.02:	+0.49:	+0.01
4702	[Fe III]	-0.23
4711+4713	[Ar IV] + He I	-0.24	+0.06
4740	[A IV]	+0.15
4861	H β	+0.57	+1.85	+1.73	+1.60	+1.55	+2.29	+2.13	+2.22	+2.11
4922+4931	He I + [O III]	-0.29	+0.38	+0.16
4959	[O III]	+1.18	+0.53	...	+2.24	+2.14	+2.33	+2.39
5007	[O III]	+0.49	+1.12	+1.68	+1.01	+0.85	+2.76	+2.62	+2.81	+2.87
5048	He I	-0.77:
5199+5201	[N I]	-0.17	-0.04	-0.30
5755	[N II]	-0.34	-0.04	-0.67
5876	He I	+0.89	+0.80	+0.72	+1.56	+1.31	+1.40	+1.24
6300	[O I]	+0.14	+0.67	+0.84	...	+0.75
6311	[S III]	-0.06	+0.60	+0.45
6364	[O I]	-0.35	+0.18	+0.31
6548	[N II]	+0.61	+1.80	+1.41	+1.60	+1.40	+1.64	...	+1.54	+0.70
6563	H α	+1.58	+2.83	+2.49	+2.57	+2.44	+3.07	+2.83	+3.04	+2.76
6583	[N II]	+1.14	+2.31	+1.84	+2.05	+1.89	+2.11	+1.89	+1.98	+1.25
6678	He I	+0.44	+1.12	+0.93	+1.17	+0.83
6717	[S II]	+0.42:	+1.89	+1.21	+1.70	+1.45	+1.68	+1.82	+1.88	+1.29
6731	[S II]	+0.69	+1.56	+1.08	+1.60	+1.27	+1.60	+1.73	+1.75	+1.19
7065	He I	+0.09	+0.98	+0.78	...	+0.89
7136	[Ar III]	+0.84	+1.56	+1.39	+1.65	+1.19
7320+7330	[O II]	+0.32	+1.18	+0.90

^a Given in log W (Å).

III. PHYSICAL CONDITIONS AND CHEMICAL COMPOSITION

a) Temperatures and Densities

The relevant references to the atomic parameters used to derive electron temperatures, electron densities, and chemical abundances are from the compilation by Mendoza (1983).

We present in Table 4 temperatures and densities derived from solutions to the forbidden line intensity ratios in the (N_e , T_e) plane. The solutions are: N_e (S II) and T (S II) from the 6717/6731 and (4068+4076)/(6717+6731) ratios, T (O III) from N_e (S II) and the 4363/5007 ratio, T (N II) from N_e (S II) and the 5755/6583 ratio, and T (O II) from N_e (S II) and the (3726+3729)/(7320+7330) ratio. The quantity $\langle T_L \rangle$ is an average of T (N II),

T (S II), and T (O II). For H40 we derived the T (O III) value based on the $\langle T_L \rangle$ value and the models by Stasinska (1982). The errors in the temperature were estimated by considering the uncertainties in the observed line intensity ratios and in the reddening corrections.

To derive the root mean square density, N_e (rms), we assumed that our observations were representative of a spherical core with $r = 3''9$ (which corresponds to the area of our rectangular entrance slit). For a homogeneous sphere of radius r and at a distance d , N_e (rms) is given by

$$N_e^2(\text{rms}) = 3d^2 I(\text{H}\beta) [1 + N(\text{He}^+)/N(\text{H}^+)] / r^3 a(\text{H}\beta, T) h\nu(\text{H}\beta), \quad (3)$$

 TABLE 4
 TEMPERATURES AND DENSITIES

REGION	T_e					N_e	
	[O III]	[N II]	[S II]	[O II]	$\langle T_L \rangle$	[S II]	(rms)
H40	< 8500 ^a	8250 ± 650	8800 ± 1000	6800 ± 700	7950	≤ 100	6.4
NGC 5461	9300 ± 250	8500 ± 550	9500 ± 1100	9500 ± 900	9150	234	14.8
NGC 5455	9800 ± 400	...	11800 ± 2300	11200 ± 1600	11500	148	7.6
NGC 5471	13400 ± 250	10800 ± 1700	12700 ± 2400	13100 ± 2000	12200	186	10.6

^a T (O III) = 7050 K was adopted for H40.

where $a(H\beta, T)$ is the $H\beta$ effective recombination coefficient. To determine $a(H\beta, T)$ we adopted a weighted average of $\langle T_L \rangle$ and $T(O III)$, given by the fraction of the volume occupied by O^+ and O^{++} , respectively, and the computations by Hummer and Storey (1987). These results are presented in Table 4.

b) Heavy Elements

To derive the ionic chemical abundances it has been assumed that the lines originate in two regions: a high-ionization zone, where the O^{++} , Ne^{++} , S^{++} , and Ar^{++} lines originate, represented by $T(O III)$, and a low-ionization zone where the O^+ , N^+ , and S^+ lines originate, represented by T_L . The exception is sulfur in H40, where S^{++} is expected to originate mostly in the O^+ zone and for which $T = 7700$ K was adopted, based on ionization structure models (Stasinska 1982; Mathis 1982, 1985). In the two zones it was assumed that there are no spatial temperature variations present, i.e., that t^2 , the mean temperature fluctuation, is equal to 0.00. The results are presented in Table 5; the errors include the uncertainties in the line intensity ratios and in the electron temperatures.

The total O, N, and Ne abundances were obtained from

$$N(O)/N(H) = N(O^+ + O^{++})/N(H^+), \quad (4)$$

$$N(N)/N(H) = [N(O)/N(O^+)] \times [N(N^+)/N(H^+)], \quad (5)$$

$$N(Ne)/N(H) = [N(O)/N(O^{++})] \times [N(Ne^{++})/N(H^+)], \quad (6)$$

and are presented in Table 6.

To determine the S and Ar total abundances we have used the ionization correction factors derived from ionization structure models by Mathis (1982, 1985) and Stasinska (1982). The errors in Table 6 include the uncertainties due to the temperatures, the line intensity ratios, and the ionization correction factors. The temperature dependence of the ionic abundances relative to H is considerably larger than that of the total abundance ratios relative to O, therefore the errors in Table 5 can be larger than those of Table 6. The S abundance for NGC 5455 is more uncertain than for the other H II regions because it is based only on the S^+ abundance and the i_{cf} provided by the ionization structure models.

c) Helium

The total helium abundance of an ionized gaseous nebula is given by

$$N(He)/N(H) = N(He^0 + He^+ + He^{++})/N(H^0 + H^+), \quad (7)$$

it can be shown that for H II regions, equation (7) can be reduced, to a high degree of approximation, to (e.g., Stasinska 1982; Peimbert, Peña, and Torres-Peimbert 1986)

$$\begin{aligned} N(He)/N(H) &= N(He^0 + He^+)/N(H^+) \\ &= i_{cf}(He) \times [N(He^+)/N(H^+)], \end{aligned} \quad (8)$$

TABLE 5
IONIC ABUNDANCES^a

Ion	H40	NGC 5461	NGC 5455	NGC 5471
N^+	7.39 ± 0.08	6.93 ± 0.08	6.64 ± 0.10	6.01 ± 0.08
O^+	8.46 ± 0.14	8.06 ± 0.12	7.82 ± 0.18	7.34 ± 0.13
O^{++}	8.08 ± 0.12	8.12 ± 0.04	8.10 ± 0.06	7.96 ± 0.02
Ne^{++}	7.36 ± 0.10	7.44 ± 0.06	7.50 ± 0.06	7.33 ± 0.04
S^+	6.09 ± 0.08	5.83 ± 0.08	5.89 ± 0.10	5.40 ± 0.09
S^{++}	6.89 ± 0.15	6.59 ± 0.10	...	6.07 ± 0.08
Ar^{++}	6.20 ± 0.10	6.03 ± 0.06	5.97 ± 0.07	5.56 ± 0.06

^a Given by $12 + \log N(X^i)/N(H^+)$.

where $i_{cf}(He)$ is the helium ionization correction factor. From the computations by Hummer and Storey (1987) and Brocklehurst (1971), and the $I(4686)/I(H\beta)$ ratio presented in Table 2 we obtained that $N(He^{++})/N(H^+) = 8 \times 10^{-4}$ for NGC 5471, an almost negligible amount of He^{++} . Moreover, it is possible that the $\lambda 4686$ feature originates in the atmospheres of WR or Of stars and not in the H II region itself; therefore in what follows we will neglect the He^{++} presence.

From the computations by Hummer and Storey (1987) and by Brocklehurst (1972) and the observations in Table 2 we have computed the $N(He^+, \lambda)/N(H^+)$ values under the assumption that the collisional excitation and the self-absorption effects from the level 2^3S of He^0 are negligible; the results are presented in Table 7. The higher $\lambda 7065$ values indicate that collisional excitation and the self-absorption effects are present. Based on the work of Peimbert and Torres-Peimbert (1987a, b) we assumed that the collisional effects from the 2^3S level are only half as large as those derived from the predictions by Berrington and Kingston (1987); i.e., we adopted a γ value of 0.50, which is equivalent to assuming that the population of the 2^3S level is only half the predicted value. After these corrections the $\lambda 7065$ values were still higher than those derived from the other helium lines, indicating the presence of self-absorption.

Based on the 7065/4472 ratios corrected for collisional excitation and the results by Robbins (1968) and Cox and Daltabuit (1971) we have taken into account the effect of self-absorption for the triplet series. This effect reduces the $(He^+, \lambda)/H^+$ ratios by at most a factor of 1.02 for $\lambda 5876$ and of 1.01 for $\lambda 4472$, while it leaves $\lambda 4026$ unaffected. From the computations by Robbins and Bernat (1973) it is found that the self-absorption effect for the singlet lines is negligible. In Table 8 we present the ionized helium abundances after correction for collisional excitation and self-absorption; from Tables 7 and 8 it can be seen that the maximum correction by these two effects is produced in NGC 2363 for $\lambda 5876$ and amounts to less than a factor of 1.04. From an expected $I(5007)/I(4933)$ [$O III$] ratio of 7.04×10^3 and the observed 5007/ $H\beta$ line intensity ratios we subtracted the 4931/ $H\beta$ contribution to the observed $(4922 + 4931)/H\beta$ ratios. In the last column of Table 8 we present the average He^+/H^+ value after considering all the lines weighted according to the observational errors (the errors given are 1σ).

The observed He and H line intensities are affected by underlying absorption and emission due to the stellar contribution to the spectra. These processes affect differently each helium line (Rayo *et al.*), since the average He^+/H^+ value of the three best observed lines $\lambda \lambda 5876, 4472, \text{ and } 6678$ is practically the same and the equivalent widths in emission of the Balmer lines are very large (see Table 3). We conclude that the effects due to underlying absorption and emission are negligible.

Table 6 includes the total He/H abundance ratios after considering the $i_{cf}(He)$ based on the ionization structure models by Mathis (1982). The correction for neutral helium for H40 depends critically on the S^{++}/S^+ ratio, an error of 0.07 dex in this ratio produces the uncertainty presented in Table 6 and in Figure 7.

Oxygen comprises about 45% by mass of the Z abundance in the Orion Nebula (Peimbert and Torres-Peimbert 1977) and about 60% in NGC 2363 (Peimbert, Peña, and Torres-Peimbert 1986). The difference is mainly due to the C/O and N/O values in NGC 2363 which are smaller than in the Orion Nebula. To derive the Z values for the M101 H II regions we assumed that O comprises from 45% to 60% of the Z value.

TABLE 6
TOTAL ABUNDANCES^a

Ratio	H40	NGC 5461	NGC 5455	NGC 5471	NGC 2363	SMC	LMC	Orion	Sun
He/H	0.0903	0.0904	0.0926	0.0797	0.077	0.078	0.084	0.102	...
12 + log O/H	8.61 ± 0.11	8.39 ± 0.08	8.28 ± 0.10	8.05 ± 0.05	7.92 ± 0.04	7.89 ± 0.08	8.34 ± 0.08	8.65 ± 0.06	8.92 ± 0.1
log C/O	-0.47 ± 0.2	-0.53 ± 0.07	-0.75 ± 0.2	-0.48 ± 0.2	-0.08 ± 0.15	-0.25 ± 0.1
log N/O	-1.07 ± 0.06	-1.13 ± 0.06	-1.18 ± 0.10	-1.33 ± 0.06	-1.48 ± 0.04	-1.48 ± 0.06	-1.31 ± 0.1	-0.97 ± 0.05	-0.93 ± 0.1
log Ne/O	-0.72 ± 0.15	-0.68 ± 0.06	-0.60 ± 0.10	-0.63 ± 0.06	-0.74 ± 0.04	-0.86 ± 0.13	-0.79 ± 0.1	-0.85 ± 0.10	-0.89 ± 0.2
log S/O	-1.64 ± 0.08	-1.69 ± 0.08	-1.55 ± 0.15	-1.67 ± 0.08	-1.60 ± 0.06	-1.53 ± 0.12	-1.58 ± 0.08	-1.55 ± 0.1	-1.69 ± 0.1
log Ar/O	-2.01 ± 0.12	-2.21 ± 0.08	-2.09 ± 0.10	-2.25 ± 0.08	-2.01 ± 0.06	-2.24 ± 0.10	-2.23 ± 0.10	-2.00 ± 0.1	-2.23 ± 0.2
Y	0.263 ^{+0.025} _{-0.012}	0.264 ± 0.007	0.269 ± 0.011	0.241 ± 0.007	0.235 ± 0.004	0.237 ± 0.006	0.250 ± 0.006	0.280 ± 0.01	...
Z	0.0111	0.0066	0.0050	0.0025	0.0017	0.0016	0.0057	0.014 ± 0.002	...
References ^b	1	1	1	1, 2	3	2, 3, 4, 5	5, 6, 7	8, 9, 10	11, 12, 13

^a By number, with the exception of Y and Z which are given by mass.

^b (1) This paper. (2) Dufour *et al.* 1984. (3) Peimbert, Peña, and Torres-Peimbert 1986. (4) Peimbert and Torres-Peimbert 1976. (5) Dufour 1984. (6) Peimbert and Torres-Peimbert 1974. (7) Lequeux *et al.* 1978. (8) Peimbert and Torres-Peimbert 1977. (9) Torres-Peimbert, Peimbert, and Dattabuit 1980. (10) Peimbert 1982. (11) Lambert 1978. (12) Lambert and Luck 1978. (13) Meyer 1985.

TABLE 7
UNCORRECTED IONIZED HELIUM ABUNDANCES^a

Region	$\lambda 4472$	$\lambda 5876$	$\lambda 6678$	$\lambda 7065$
H40	0.072	0.068	0.070	0.085
NGC 5461	0.083	0.093	0.091	0.170
NGC 5455	0.102	0.089	0.079	0.135
NGC 5471	0.076	0.087	0.085	0.151
NGC 2363	0.078	0.078	0.078	0.155

^a Given by $N(\text{He}^+)/N(\text{H}^+)$, without correction for self-absorption nor for collisional excitation from the 2^3S He^0 level.

The value for each object was obtained by adopting the N/O ratio as the interpolating factor. A result that supports this procedure is the uniformity of the C/N ratio in galactic and extragalactic H II regions with very different O/H ratio (e.g., Dufour *et al.* 1984; Peimbert 1985 and references therein).

IV. DISCUSSION

For the same objects in M101 we obtain higher temperatures and lower O/H abundances than those derived by other authors from observations with IDS detectors, the comparison is made assuming $t^2 = 0.00$ for all observations; the main differences are due to the nonlinearity of the IDS detectors and not to the accuracy of the observed intensity ratios (like 4363/5007). For H40, NGC 5461, and NGC 5471 the derived difference is of the order of 0.2 dex relative to the results by Smith (1975) and by Rayo *et al.* Many of the direct O/H determinations in the literature are based on IDS observations and consequently should be decreased on the average by about 0.2 dex.

In Figure 1 we present our oxygen determinations for H II regions in M101 and those by Rayo *et al.* for $t^2 = 0.00$. We have also recomputed the O/H values from the uncorrected observations by Smith (1975) for $t^2 = 0.00$; these values are also shown in the same figure. Moreover in Figure 1 we present the oxygen values derived by Dopita and Evans (1986) from their grid of ionization structure models. Their results agree with the direct O/H determinations based on *uncorrected IDS observations* for values of $[12 + \log(\text{O}/\text{H})] < 8.8$ but are systematically higher than our results by about 0.2 dex.

The difficulty of directly measuring T_e led Pagel *et al.* (1979) to propose an empirical method based on the nebular oxygen lines $([\text{O II}] \lambda 3727 + [\text{O III}] \lambda \lambda 4959, 5007)/\text{H}\beta$ to determine the electron temperature and the O/H ratio. In Figure 2 we present three of the most recent calibrations based on the empirical method (Edmunds and Pagel 1984; McCall *et al.*; Dopita and Evans 1986). For comparison we present in the same figure our results for M101 as well as those for NGC 2363 (Peimbert, Peña, and Torres-Peimbert 1986) based on direct determinations of the O/H ratios assuming $t^2 = 0.00$. It can be

TABLE 8

CORRECTED IONIZED HELIUM ABUNDANCES^a

Region	$\lambda 4026$	$\lambda 4472$	$\lambda 4922$	$\lambda 5876$	$\lambda 6678$	Average
H40	0.072	0.072	0.068	0.070	0.070 ± 0.004
NGC 5461	0.079	0.083	0.092	0.092	0.091	0.088 ± 0.004
NGC 5455	0.089	0.102	...	0.088	0.079	0.092 ± 0.005
NGC 5471	0.072	0.074	0.082	0.085	0.085	0.080 ± 0.003
NGC 2363	0.076	0.076	0.075	0.075	0.077	0.076 ± 0.002

^a Given by He^+/H^+ corrected for self-absorption and for collisional excitation from the 2^3S He^0 level.

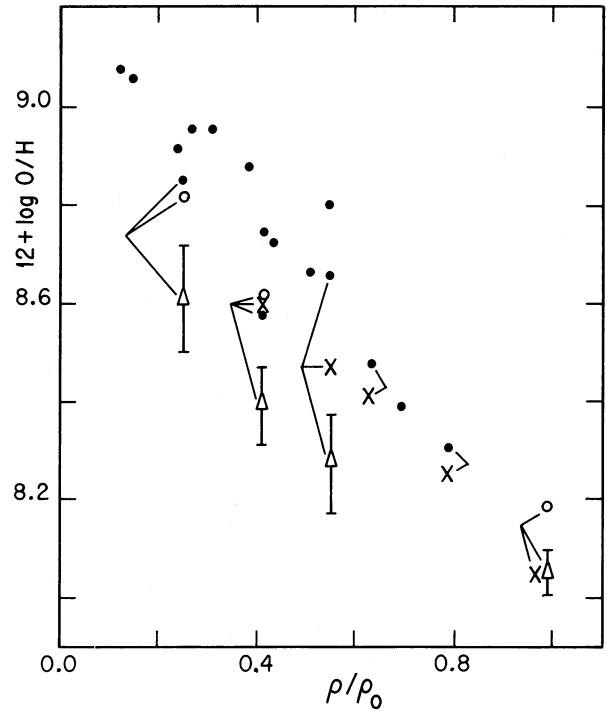


FIG. 1.—O/H vs. galactocentric distance, where we have adopted $\rho/\rho_0 = 0.99$ for NGC 5471. Triangles are from this paper, open circles from Rayo *et al.*, crosses from Smith (1975), and filled circles from Evans (1986). O/H values of the same object determined by different authors are connected by thin lines.

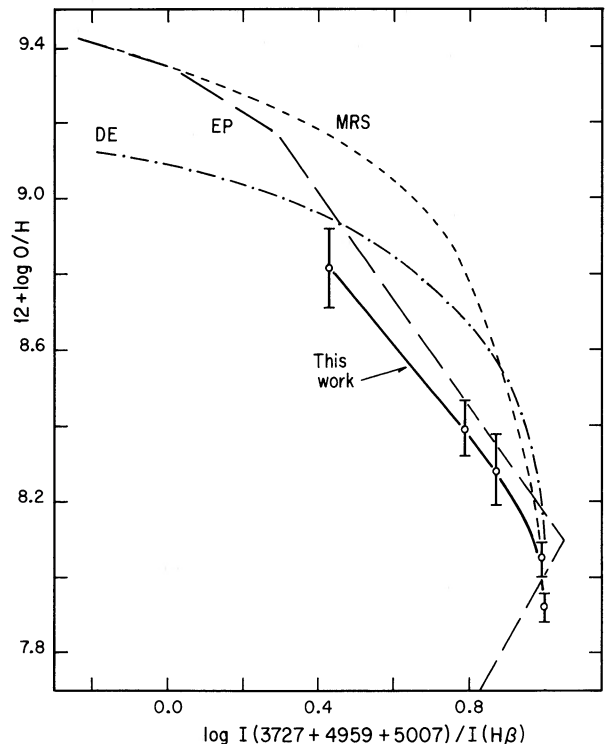


FIG. 2.—We present the empirical relations by Edmunds and Pagel (1984), McCall *et al.* (1985), and Dopita and Evans (1986) between O/H and the $([\text{O II}] \lambda 3727 + [\text{O III}] \lambda \lambda 4959, 5007)/\text{H}\beta$ intensity ratio. Also in this figure we present our results for M101 based on direct O/H determinations.

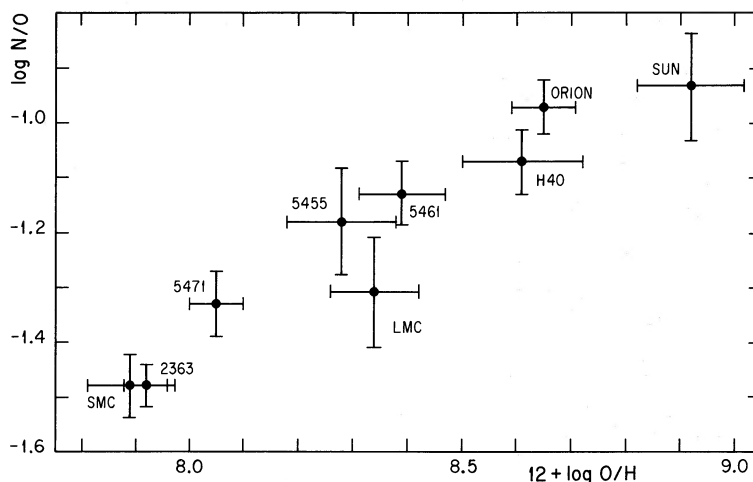


FIG. 3.—N/O vs. O/H ratio of the objects listed in Table 6

seen that our O/H results agree fairly well with the calibration by Edmunds and Pagel (1984) that is based also on observations and $t^2 = 0.00$, but are considerably smaller than those predicted by the calibrations by McCall *et al.* and by Dopita and Evans (1986) that are based on models.

Part of the O/H difference between the models and the observations is due to the presence of temperature inhomogeneities over the observed volumes that imply t^2 values different from zero (e.g., Peimbert 1967; Peimbert and Costero 1969), the t^2 effect should be studied to evaluate whether it can explain most of the difference.

A relationship of the type $\log(N/O) = a \log(O/H) + b$ with $a = 1$ is predicted by the simple model of galactic chemical evolution for the interstellar medium under the assumptions that N is of secondary origin and O is of primary origin (e.g., Talbot and Arnett 1973). The simple model is based on the following assumptions: (a) there are no gas flows, (b) the initial mass function is constant with time, and (c) the instant recycling approximation applies. In Figure 3 we present a plot of the N/O versus O/H ratios for the objects listed in Table 6. From our data we derive that $a = 0.46 \pm 0.1$. This result implies that an important fraction of N is not of secondary origin or that the simple model of galactic chemical evolution does not apply, or both. Similar values for a have been obtained before by other authors and different models of galac-

tic chemical evolution have been proposed to explain the observations (e.g., Peimbert 1987 and references therein). The Orion Nebula and the Sun follow smoothly the M101 H II regions, probably implying that the chemical evolutions of the Galaxy and of M101 have not been very different.

We present the Ne/O ratio, as derived from equation (6), versus the O/H values for the observed objects in Figure 4. From ionization structure models it has been found that equation (6) breaks down for H II regions of low degree of ionization (see also Fig. 4 in Torres-Peimbert and Peimbert 1977); we suggest that this effect is also present in our sample since H40 and Orion show slightly lower Ne/O values than the other objects in M101. We find no evidence for a Ne/O gradient in M101, and we conclude that all objects in our sample are consistent with a constant ratio given by $\log \text{Ne/O} = -0.70 \pm 0.10$. The SMC and LMC H II regions show marginally smaller Ne/O ratios than NGC 2363 and M101; this difference is not due to the nonlinearity correction of the O/H ratios since the Ne/H ratios are similarly affected.

In Figure 5 we present the S/O versus O/H ratios for the H II regions in M101. Our results indicate that there is no variation of the S/O ratio with galactocentric distances and that $\log(S/O) = -1.60 \pm 0.10$ for all objects, in agreement with the idea that the sulfur and oxygen enrichment is due to stars of similar mass. Our results are in disagreement with the results

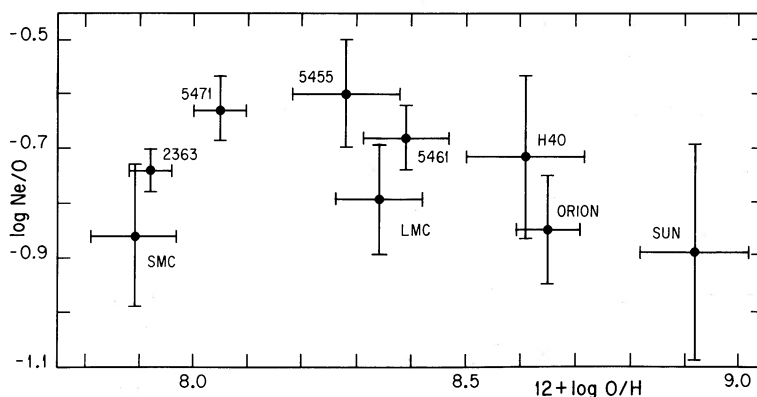


FIG. 4.—Ne/O vs. O/H values for the objects listed in Table 6. The Ne/O ratio was derived from eq. (6); this equation breaks down for objects of low degree of ionization. We find no evidence for a Ne/O gradient in M101.

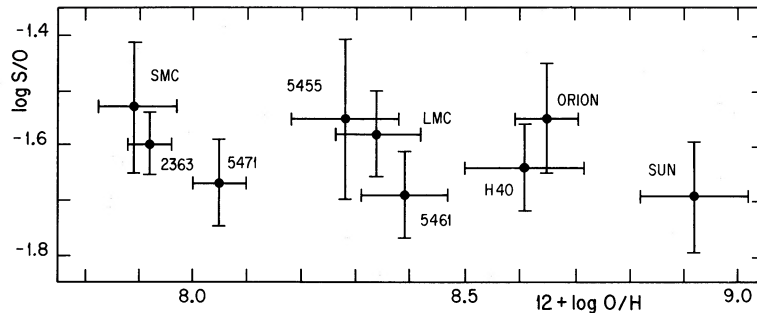


FIG. 5.—S/O vs. O/H ratio for the objects listed in Table 6. Our results indicate that there is no variation of the S/O ratio with galactocentric distance in M101 and that $\log(S/O) = -1.60 \pm 0.10$ for all objects; in agreement with the idea that the S and O enrichment is due to stars of similar mass.

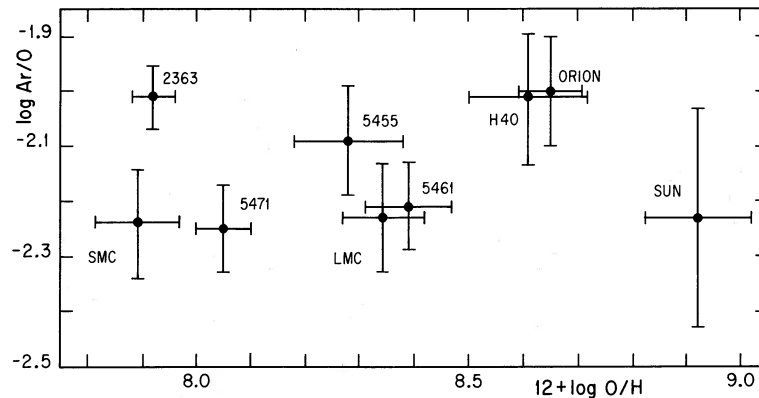


FIG. 6.—Ar/O vs. O/H ratio for the objects listed in Table 6. Our results are consistent with a constant ratio given by $\log(Ar/O) = -2.15 \pm 0.15$.

for M101 by Evans (1986), for M33 by Vilchez *et al.* (1988), and for the Galaxy by Shaver *et al.* (1983) who find an S/O gradient increasing with galactocentric distance. For M101 we consider that our observations are of higher quality, while for M33 and the Galaxy we consider that more accurate observations are needed to confirm the published results. We display argon versus oxygen in Figure 6. Again our results are consistent with a constant ratio given by $\log(Ar/O) = -2.15 \pm 0.15$.

In Figure 7 we present the helium versus oxygen diagram. In addition to the values in Table 6 we have added the M17 results by Peimbert *et al.* (1988). There are systematic differences between the helium abundances derived by us and those by Rayo *et al.* mainly due to the nonlinearity of the IDS. The difference amounts to $\Delta Y = 0.015$, in the sense that the present values are higher.

As a first approximation to the study of the chemical enrichment of the interstellar medium it has been assumed that there is a linear relation between the helium mass fraction, Y , and the heavy element mass fraction, Z of the form

$$Y = Y_p + Z(\Delta Y/\Delta Z), \quad (9)$$

where Y_p denotes the pregalactic helium abundance (e.g., Peimbert and Torres-Peimbert 1974, 1976).

Based on equation (9) and observations of the SMC H II regions and the Orion Nebula gathered with a linear detector Peimbert and Torres-Peimbert (1976) found that $Y_p = 0.228$.

A few years of depression for Y_p followed since French (1980), Talent (1980), and Rayo *et al.* obtained $Y_p = 0.216$. These values should be corrected for the nonlinearity of the detectors used. The correction to be applied yields a higher helium abundance by about 0.015.

Kunth and Sargent (1983) obtained an average helium abundance $\langle Y \rangle = 0.245 \pm 0.003$ (1σ) from 13 extragalactic H II regions. Kunth and Sargent proposed that $Y_p = \langle Y \rangle$, i.e., that $\Delta Y/\Delta Z = 0$ in equation (9). By contrast, Pagel (1986) from the data by Kunth and Sargent, and by disregarding one object in

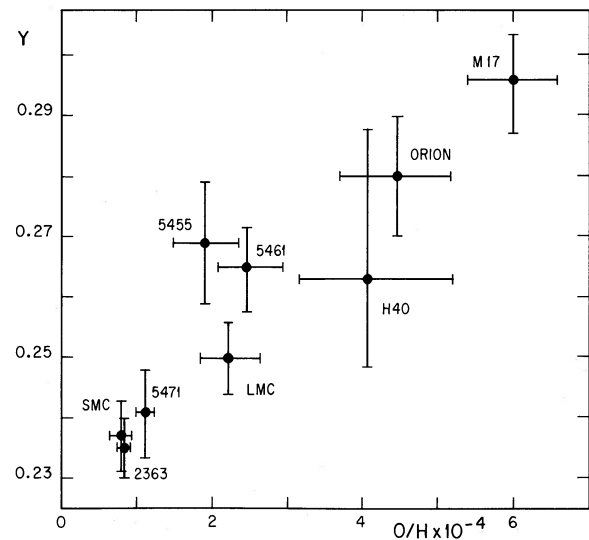


FIG. 7.—O/H vs. Y for the objects listed in Table 6. In addition to the values in this table we have added the values of M17 by Peimbert *et al.* (1988). The difference between the helium abundances derived by Rayo *et al.* and those derived by us is mainly due to the nonlinearity of the IDS. The difference amounts to $\Delta Y = 0.015$, in the sense that the present values are higher.

their sample, derived $Y_p = 0.234 \pm 0.008$ and $\Delta Y/\Delta Z = 4.6 \pm 5.9$. From independent observational data Pagel, Terlevich, and Melnick (1986) found $Y_p = 0.236 \pm 0.005$ and $\Delta Y/\Delta Z = 5.7 \pm 2.7$. These results were derived without correcting for self-absorption nor for collisional excitation from the 2^3S level and consequently are upper limits to Y_p . The models of chemical evolution of galaxies, and in particular $\Delta Y/\Delta Z$, depend on at least four different parameters that are not well known: (a) gas flows, often characterized by the ratios of the infall and outflow rates to the star-formation rate, (b) the initial mass function (and its time dependence), (c) the star-formation rate (and its time dependence), and (d) the mass and composition of the stellar ejecta during the evolution of stars of different masses. Therefore the approximation in equation (9) might not be valid and the relation between Y and Z is not necessarily linear.

It should be mentioned that almost always the Z values in equation (9) have been based on the O abundance alone, and that equation (9) has been substituted by

$$Y = Y_p + X_O(\Delta Y/\Delta X_O), \quad (10)$$

where X_O is the O abundance by mass. Similar expressions can be set up for C and N. The Y_p values derived from the four similar relations will be denoted by $Y_p(Z)$, $Y_p(O)$, $Y_p(C)$, and $Y_p(N)$. In Table 9 we present the $Y_p(Z)$, $Y_p(O)$, $Y_p(C)$, and $Y_p(N)$ values derived from the NGC 5471 and the Orion Nebula values. Almost the same values would have been obtained by combining the results of NGC 5471 with those for M17 presented by Peimbert *et al.* (1988). Also in Table 9 we show the values derived from NGC 2363, and the SMC regions, together with the Orion Nebula. The different Y_p values derived for the same objects are significant and imply that at least two of the four relations used are nonlinear.

Other authors have also presented $Y_p(N)$ and $Y_p(C)$ values: Pagel *et al.* from their sample of H II regions obtained that $Y_p(N) = 0.238 \pm 0.005$ (1 σ), without correcting for collisional excitation nor self-absorption from the 2^3S level; Gallagher, Steigman, and Schramm (1987) from data available in the literature obtained $Y_p(C) = 0.235 \pm 0.004$ (1 σ), without correction for collisional excitation from the 2^3S level; Pagel (1988) analyzing part of the data available in the literature and new unpublished data derived $Y_p(O) = 0.230 \pm 0.005$ (1 σ) and $Y_p(N) = 0.232 \pm 0.004$ (1 σ).

To select the best Y_p value from those presented in Table 9 in what follows we will discuss whether the helium enrichment behaves linearly with any of Z , O, N or C. According to Sarmiento and Peimbert (1985) more than 60% and possibly as much as 80% of C is produced in intermediate mass stars, those with $1 < M/M_\odot < 8$; the rest is produced by massive stars, those with $M > 8 M_\odot$. Alternatively, most of the O is produced by massive stars. From stellar evolution models Serrano and Peimbert (1981) find that He is produced by intermediate-mass stars and by massive stars; on observational

grounds there are three types of objects that enrich the interstellar medium with large amounts of He: (a) PN of Type I (e.g., Peimbert 1987), (b) WN stars (e.g., Parker 1978; Kwitter 1981), and (c) supernovae of the Crab Nebula type (e.g., Péquignot and Dennefeld 1983; Davidson and Fesen 1985; Henry 1986; MacAlpine *et al.* 1989). Of these three types of objects only the first two are also N-rich. If He is produced on the average by stars with smaller mass than those that produce O, it can be shown (i.e., Serrano and Peimbert 1981) that objects with a high star-formation rate would yield a $Y_p(O)$ value lower than the real Y_p value, i.e., $Y_p(O) < Y_p(\text{true})$.

Pagel (1986), based on a correlation between the N and He abundances in irregular and blue compact galaxies of low O abundance and on the presence of WN features in their spectra, suggested that most of the N in these objects was of secondary origin but produced by massive WN stars. If we assume that all the helium additional to Y_p and all the N are produced by massive stars and that N is of secondary origin, then $\Delta X_N \propto (X_C + X_O)\Delta Y \propto \Delta Y^n$, where n is larger than 1 and is equal to 2 if $(X_C + X_O) \propto \Delta Y$ (Pagel 1986; Peimbert 1987). The values $Y_p(N)$ derived from a linear extrapolation of ΔX_N versus ΔY become upper limits to the real Y_p values (see Fig. 1 of Peimbert 1987), i.e., $Y_p(N) > Y_p(\text{true})$.

As mentioned before the C/N ratio appears to be uniform in H II regions of different O/H content implying that $Y_p(N) = Y_p(C)$; therefore the delay in the C and N enrichment of the interstellar medium is similar and since C is a primary element we conclude that C is produced by stars with an average mass smaller than those that produce N.

From our discussion it follows that $Y_p(O) < Y_p(N) = Y_p(C)$ in agreement with the values in Table 9. Moreover it also follows that $Y_p(O) < Y_p(\text{true}) < Y_p(N) = Y_p(C)$. Most of the He enrichment of the interstellar medium is expected to be due to massive stars. Nevertheless a small nonnegligible fraction comes from intermediate mass stars; therefore a better approximation than $Y_p(O)$ or $Y_p(C)$ to derive $Y_p(\text{true})$ is given by $Y_p(Z)$.

Based on this discussion it follows that from NGC 5471 we obtain $Y_p = 0.232 \pm 0.008$ (1 σ), from NGC 2363, $Y_p = 0.228 \pm 0.006$ (1 σ), and from the SMC H II regions, $Y_p = 0.232 \pm 0.005$ (1 σ). The corrections by self-absorption and collisional de-excitation from the 2^3S level have not been considered for the SMC H II regions, but they are small and would reduce Y_p to about 0.229. For NGC 2363 the corrections for collisional excitation amount to less than 0.001 and have not been considered.

V. CONCLUSIONS

We present line intensity ratios for a group of H II regions in M101 observed with an IDS detector after correcting for non-linearity. By comparing our results with those determined with IDS detectors without correcting by this effect we find significant and systematic changes in $C(H\beta)$, T_e , O/H, and Y_p : the $C(H\beta)$ values derived by us are about 0.15 dex smaller, the T_e values are a few hundred degrees higher, the O/H values are about 0.2 dex smaller, and the Y_p values are about 0.015 higher. As it has been discussed elsewhere (Peimbert and Torres-Peimbert 1987a) it is not possible to correct properly for the nonlinearity effect based only on the published line intensity ratios, it is necessary to reduce the data again from the original measurements.

The O/H ratios derived from the observed T_e values are in good agreement with the empirical calibration of the $([O III] + [O II])/H\beta$ versus O/H ratio by Edmunds and Pagel

TABLE 9
PREGALACTIC HELIUM ABUNDANCE^a

Region	$Y_p(O)$	$Y_p(C)$	$Y_p(N)$	$Y_p(Z)$
NGC 5471	0.228	0.237	0.236	0.232
NGC 2363	0.225	0.232	0.232	0.228
SMC	0.228	0.235	0.235	0.231

^a By mass.

(1984) but are smaller than those derived from the calibrations by Dopita and Evans (1986) and by McCall *et al.*, part of the difference is due to spatial temperature variations over the observed volumes.

We found gradients in the T_e , He/H, O/H, and N/O values with galactocentric distance. The N/O gradient implies that the history of the N chemical enrichment is different to that of O, and that probably a significant fraction of N is of secondary origin.

Contrary to previous results we do not find gradients in the S/O, Ne/O, and Ar/O ratios implying that the history of the O, Ne, S, and Ar enrichment is similar and that stars in the same mass range are responsible for most of their production.

We computed the effects of self-absorption and collisional excitation from the He I 2^3S level for giant extragalactic H II regions. The combined effects reduce the helium abundances derived from the $\lambda 5876$ lines by at most a factor of 1.04, from

the $\lambda 4472$ lines by at most a factor of 1.02, and from the $\lambda 6678$ lines by at most a factor of 1.01; moreover for $\lambda\lambda 4026$ and 4922 these effects are completely negligible.

We find that a linear relationship of the type $Y = Y_p + X\Delta Y/\Delta X$, where X could be Z , X_C , X_N , or X_O yield different values of Y_p , which we have designated $Y_p(Z)$, $Y_p(C)$, $Y_p(N)$, and $Y_p(O)$. It is argued that the real Y_p value is smaller than $Y_p(N)$ and $Y_p(C)$, but larger than $Y_p(O)$. Therefore it is suggested that $Y_p(Z)$ provides the best representation of the pregalactic helium abundance.

From this discussion and the results for M17, the Orion Nebula, NGC 5471, NGC 2363, and the SMC H II regions it follows that $Y_p = 0.230 \pm 0.006$ (1 σ).

We are grateful to the staff of the Kitt Peak National Observatory for their excellent support to this program, and in particular to J. Barnes and J. B. DeVeney for their assistance.

REFERENCES

- Berrington, K. A., and Kingston, A. E. 1987, *J. Phys. B.*, **20**, 6631.
 Brocklehurst, M. 1971, *M.N.R.A.S.*, **153**, 471.
 ———. 1972, *M.N.R.A.S.*, **157**, 211.
 Cox, D. P., and Daltabuit, E. 1971, *Ap. J.*, **167**, 257.
 Davidson, K., and Fesen, R. A. 1985, *Ann. Rev. Astr. Ap.*, **23**, 119.
 de Vaucouleurs, G. 1978, *Ap. J.*, **223**, 351.
 Dopita, M. A., and Evans, I. N. 1986, *Ap. J.*, **307**, 431.
 Dufour, R. J. 1984, in *IAU Symposium 108, Structure and Evolution of the Magellanic Clouds*, ed. S. van den Bergh and K. S. de Boer (Dordrecht: Reidel), p. 353.
 Dufour, R. J., Schiffer, F. H., III, and Shields, G. A. 1984, in *Future of Ultraviolet Astronomy Based on Six Years of IUE Research*, ed. J. M. Mead *et al.* (NASA CP-2349), p. 111.
 Edmunds, M. G., and Pagel, B. E. J. 1984, *M.N.R.A.S.*, **211**, 507.
 Evans, I. N. 1986, *Ap. J.*, **309**, 544.
 French, H. B. 1980, *Ap. J.*, **240**, 41.
 Gallagher, J. S., Steigman, G., and Schramm, D. 1987, in *13th Texas Symposium on Relativistic Astrophysics*, ed. M. P. Ulmer (Singapore: World Scientific), p. 203.
 Henry, R. B. C. 1986, *Pub. A.S.P.*, **98**, 1044.
 Hodge, P. W. 1969, *Ap. J. Suppl.*, **18**, 73.
 Hummer, D. G., and Storey, P. J. 1987, *M.N.R.A.S.*, **224**, 801.
 Kunth, D., and Sargent, W. L. W. 1983, *Ap. J.*, **273**, 81.
 Kwitter, K. B. 1981, *Ap. J.*, **245**, 154.
 Lambert, D. L. 1978, *M.N.R.A.S.*, **182**, 249.
 Lambert, D. L., and Luck, R. E. 1978, *M.N.R.A.S.*, **183**, 79.
 Lequeux, J., Peimbert, M., Rayo, J. F., Serrano, A., and Torres-Peimbert, S. 1979, *Astr. Ap.*, **80**, 155.
 MacAlpine, G. M., McGaugh, S. S., Mazzarella, J., and Uomoto, A. 1989, *Ap. J.*, **342**, 364.
 McCall, M. L., Rybski, P. M., and Shields, G. A. 1985, *Ap. J. Suppl.*, **57**, 1.
 Mathis, J. S. 1982, *Ap. J.*, **261**, 195.
 ———. 1985, *Ap. J.*, **291**, 247.
 Mendoza, C. 1983, in *IAU Symposium 103, Planetary Nebulae*, ed. D. R. Flower (Dordrecht: Reidel), p. 143.
 Meyer, J. P. 1985, *Ap. J. Suppl.*, **57**, 151.
 Oke, J. B. 1974, *Ap. J. Suppl.*, **27**, 21.
 Pagel, B. E. J. 1986, in *Advances in Nuclear Astrophysics*, ed. E. Vangioni-Flam *et al.* (Gif/Yvette: Editions Frontières), p. 53.
 Pagel, B. E. J. 1988, in *A Unified View of the Macro- and Micro-Cosmos*, ed. A. de Rújula, D. Nanopoulos, and P. A. Shaver (Singapore: World Scientific), p. 399.
 Pagel, B. E. J., Edmunds, M. G., Blackwell, D. E., Chun, M. S., and Smith, G. 1979, *M.N.R.A.S.*, **189**, 95.
 Parker, B. E. J., Terlevich, R. J., and Melnick, J. 1986, *Pub. A.S.P.*, **98**, 1005.
 Peimbert, R. A. R. 1978, *Ap. J.*, **224**, 873.
 Peimbert, M. 1967, *Ap. J.*, **150**, 825.
 ———. 1982, *Ann. N.Y. Acad. Sci.*, **395**, 24.
 ———. 1985, in *Star Forming Dwarf Galaxies and Related Objects*, ed. D. Kunth, T. X. Thuan, and J. Tran Thanh Van (Gif/Yvette: Editions Frontières), p. 403.
 ———. 1987, in *Planetary and Proto-Planetary Nebulae: From IRAS to ISO*, ed. A. Preite-Martinez (Dordrecht: Reidel), p. 91.
 Peimbert, M., and Costero, R. 1969, *Bol. Obs. Tonantzintla y Tacubaya*, **5**, 3.
 Peimbert, M., Peña, M., and Torres-Peimbert, S. 1986, *Astr. Ap.*, **158**, 266.
 Peimbert, M., and Spinrad, H. 1970, *Astr. Ap.*, **7**, 311.
 Peimbert, M., and Torres-Peimbert, S. 1974, *Ap. J.*, **193**, 327.
 ———. 1976, *Ap. J.*, **203**, 581.
 ———. 1977, *M.N.R.A.S.*, **179**, 217.
 ———. 1987a, *Rev. Mexicana Astr. Af.*, **14**, 540.
 ———. 1987b, *Rev. Mexicana Astr. Af.*, **15**, 117.
 Peimbert, M., Ukita, N., Hasegawa, T., and Jugaku, J. 1988, *Pub. Astr. Soc. Japan*, **40**, 581.
 Péquignot, D., and Dennefeld, M. 1983, *Astr. Ap.*, **120**, 249.
 Rayo, J. F., Peimbert, M., and Torres-Peimbert, S. 1982, *Ap. J.*, **255**, 1.
 Robbins, R. R. 1968, *Ap. J.*, **151**, 511.
 Robbins, R. R., and Bernat, A. P. 1973, *Mém. Soc. Roy. Sci. Liège*, 6th Ser., **5**, 263.
 Sandage, A., and Tammann, G. A. 1976, *Ap. J.*, **210**, 7.
 Sarmiento, A., and Peimbert, M. 1985, *Rev. Mexicana Astr. Af.*, **11**, 73.
 Searle, L. 1971, *Ap. J.*, **168**, 327.
 Searle, L., and Sargent, W. L. W. 1972, *Ap. J.*, **173**, 25.
 Sedwick, K. E., and Aller, L. H. 1981, *Proc. Nat. Acad. Sci. USA*, **78**, 1994.
 Serrano, A., and Peimbert, M. 1981, *Rev. Mexicana Astr. Af.*, **5**, 109.
 Shaver, P. A., McGee, R. X., Newton, L. M., Danks, A. C., and Pottasch, S. R. 1983, *M.N.R.A.S.*, **204**, 53.
 Shields, G. A., and Searle, L. 1978, *Ap. J.*, **222**, 821.
 Smith, H. E. 1975, *Ap. J.*, **199**, 591.
 Stasinska, G. 1982, *Astr. Ap. Suppl.*, **48**, 299.
 Stone, R. P. S. 1977, *Ap. J.*, **218**, 767.
 Talbot, R. J., Jr., and Arnett, W. D. 1973, *Ap. J.*, **186**, 51.
 Talent, D. L. 1980, Ph.D. thesis, Rice University.
 Torres-Peimbert, S., and Peimbert, M. 1977, *Rev. Mexicana Astr. Af.*, **2**, 181.
 Torres-Peimbert, S., Peimbert, M., and Daltabuit, E. 1980, *Ap. J.*, **238**, 133.
 Vilchez, J. M., Pagel, B. E. J., Díaz, A. I., Terlevich, E., and Edmunds, M. G. 1988, *M.N.R.A.S.*, **235**, 633.
 Whitford, A. E. 1958, *A.J.*, **63**, 201.

J. FIERRO, M. PEIMBERT, and S. TORRES-PEIMBERT: Instituto de Astronomía, Universidad Nacional Autónoma de México, Apartado Postal 70-264, México 04510, D. F. México